MONTANA STATE UNIVERSITY

Nonaqueous organometallic electrochemistry : heterogeneous coupling of alkyl halides with reduced iron

by Jeffrey Louis Hall

A thesis submitted in partial fulfillment of the requirements for the degree of DOCTOR OF PHILOSOPHY in Chemistry
Montana State University
© Copyright by Jeffrey Louis Hall (1977)

Abstract:
The electrochemical reduction of an N,N'-dimethylformamide, DMF, solution of iron (III) acetylacetonate, Fe(acac)3 , in the presence of 1-octyl bromide has been investigated. The strategy for the reaction is to selectively reduce the metal ion to a lower valent state without concomitant electrochemical reduction of the organic halide. The 1-octyl bromide was converted to octane, 1-octene, and hexadecane.

Electrolysis cells were operated with either a constant applied potential across two aluminum electrodes or with potentiostatic control of the working electrode potential. The latter cell required the generation of a stable reference electrode suitable for use in DMF. The cadmium amalgam reference electrode was such a reference.

The yields of hexadecane ranged from 0 to 33% for identically assembled two-electrode cells operating with a 1.5 volts applied across two aluminum electrodes. Potentiostatic control of the working electrode potential was hoped to decrease the wide range in yields of coupled product, however, this did not occur. Using an aluminum working electrode in identically assembled three-electrode electrolysis cells operating with the working electrode potential held at -0.9V vs Cd(Hg), the yields of hexadecane ranged from 35 to 59%.

The current-time behavior for the reduction of Fe(acac)3 in the presence of 1-octyl bromide using aluminum electrodes was recorded for both the two-electrode and three-electrode electrolysis cells. The current increased steadily with time for the two-electrode cell run at constant applied potential before falling to near zero levels. This is unusual for a simple reduction. The three-electrode cell held at a constant working electrode potential of -0.9V vs Cd(Hg) generated two current transients. The first current transient was generated as a result of iron plating onto the aluminum working electrode. The overpotential for reducing iron ions at an iron surface is less than the overpotential for the same reduction at aluminum, therefore the increase in current. The second current transient is assigned to the formation of an organoiron which is also electroactive.

The conversion of 1-octyl bromide to hexadecane, octane, and 1-octene is a one-electron heterogeneous reaction occurring at an iron-plated surface. The 1-octyl bromide is suggested to oxidatively add or dissociative!y adsorb onto the active iron surface. A one-electron transfer occurs expelling a bromide ion. This corresponds to the second current transient. Products are formed as a result of free radical reactions. The reaction is sensitive to the pretreatment of the aluminum electrodes, total cell current, and the nature of the plated iron surface. An epitaxial effect by the aluminum electrode is suggested to account for these observations.

42

NONAQUEOUS ORGANOMETALLIC ELECTROCHEMISTRY: HETEROGENEOUS COUPLING OF ALKYL HALIDES WITH REDUCED IRON

by

JEFFREY LOUIS HALL

A thesis submitted in partial fulfillment
of the requirements for the degree

of

DOCTOR OF PHILOSOPHY

in

Chemistry

Approved:

P. W. Jennings
Chairperson, Graduate Committee

E. W. Anacker
Head, Major Department

Henry L. Parsons
Graduate Dean

MONTANA STATE UNIVERSITY
Bozeman, Montana

April, 1977

to Karen and Sarah,

who made it all worthwhile

"Brevity, the soul of wit,

may become the very body of untruth."

A. Huxley

ACKNOWLEDGMENTS

My indebtedness to several individuals extends beyond a singular acknowledgment, but that is all that I can publicly offer while privately extending my friendship and respect. I hope that this humble offering is accepted.

George W. Keulks first introduced me to scientific research and heterogeneous catalysis. The offer he extended to me to work with him and his group was a turning point in my career. As a research director, instructor, and friend, he commands those faculties that make a great professional and provides a sound example to emulate. He has fired my zeal for heterogeneous catalysis.

Richard D. Geer has listened to my tales of electrochemistry and organometallic interactions, investing long and unrewarded hours of his own time. Without his timely contribution of a three-electrode potentiostat to this effort, the research might still be idling in the dark ages of the two-electrode constant applied potential cell. Bradford P. Mundy has sounded out my love for chemistry and kept the fires kindled through friendship and understanding. Arnold C. Craig developed a level of professionalism in me that can only come from a professional. I wish to thank Reed A. Howald for his stimulating tutorship in quantum mechanics and ligand field theory plus his willingness to instruct me in the ways of the dry fly. I wish to thank my

advisor, P. W. Jennings, for his support during this project. The graduate research assistantships he acquired for me during the course of this research effort helped accelerate the development of this project. To all of these individuals, thank you for increasing my understanding.

A thank you is also extended to two individuals who assisted with the analytical examination of the surface of the iron-plated aluminum working electrode. James Campbell obtained the X-ray fluorescent spectrum of the surface of the electrode while Phil McCandless obtained the scanning electron micrographs.

None of this would have been possible had I not had such proud, loving parents to be examples for me throughout my life. They have taught me to love and respect my Lord, my fellow man, and myself. I can never hope to repay them; all that I can do is give unto my family what they have given unto me.

TABLE OF CONTENTS

	Page
DEDICATION	i
FRONTISPIECE	ii
TITLE PAGE	iii
VITA	iv
ACKNOWLEDGMENTS	v
TABLE OF CONTENTS	vii
LIST OF TABLES	ix
LIST OF FIGURES	xii
ABSTRACT	xv
INTRODUCTION	1
General Group VIII Transition Metal Chemistry	2
Iron Chemistry	10
Iron (-II)	10
Iron (0)	13
Iron (I)	19
Iron (II)	25
Iron (III)	30
Reduction of Organic Halides	32
Organometallic Electrochemistry	37
Electrochemical Cells	41
Statement of the Problem	43
DISCUSSION	44
Two-Electrode Systems	44

Page

Three-Electrode Electrolysis 64
Reference Electrode 66
Potentiostat 76

Potentiometry 78

Current-Time Behavior 81

Components of the Electrolysis Cell 100

Electrodes and Cell Design 101

Electrode History 129

Base Electrolyte 134

Solution Components 142

Total Current 144

Spectroscopic Studies 147

Homogeneous vs Heterogeneous 159

Product Formation vs Time 174

Intermediates 181

Other Substrates 184

SUMMARY 188

EXPERIMENTAL 195

BIBLIOGRAPHY 209

APPENDIX 221

LIST OF TABLES

Table		Page
I.	Classification of Ligands on the Basis of Donated Electrons (8)	3
II.	Comparison of Coordination Chemistry and Organic Chemistry Intermediates (7)	7
III.	Cathode Potential versus Product Distribution (90)	38
IV.	Coupling of Organic Halides (105)	45
V.	Approximate Exchange Current Densities for the Hydrogen Reaction on Metals at 25°C (108)	55
VI.	Product Yields for the Two-Electrode Constant Applied Potential Electrolysis Cell with Octyl Bromide and $Fe(acac)_3$ using Aluminum Electrodes	57
VII.	Glassy Carbon Reference, $E_{1/2}$ of Ni(II) in 1.0M KCl	71
VIII.	Comparison of Reference Electrodes (124)	75
IX.	Half-wave Potentials for $Fe(acac)_3$ and $n\text{-}C_8H_{17}Br$	79
X.	Effect of Cathode Material on Reduction of $(C_6H_5CH_2)(C_2H_5)_3NNO_3$ in DMF (141,143)	102
XI.	Three-Electrode Cell Examination of the Aluminum Alloys	104
XII.	Three-Electrode Cell Examination of Other Electrode Materials	106
XIII.	Macroelectrolysis Cell Breaking Potentials for $1\text{-}C_8H_{17}Br$	108
XIV.	Blank Reactions with the Three-Electrode Cell	110

Table		Page
XV.	Reduction of $Fe(acac)_3$ at Mixed Electrodes with Three-Electrode Cell	117
XVI.	Platinum Counter Electrodes in Three-Electrode Cell	124
XVII.	Solubility and Specific Resistances for R_4NX Salts in DMF (96)	136
XVIII.	Effects of Base Electrolytes	139
XIX.	Added Inorganic Base Electrolytes	141
XX.	Effects of Varying the Concentration of Ph_3P and $n\text{-}C_8H_{17}Br$	143
XXI.	Total Current Effects on Three-Electrode Cell	146
XXII.	λ_{max} for $Fe(acac)_3$ and Reduced Forms (162)	150
XXIII.	Spectral Properties of an Electrolyzed 1-Octyl Bromide Free Solution	151
XXIV.	Spectral Properties of Solutions with a Pt Counter Electrode	157
XXV.	Homogeneous vs Heterogeneous Reaction	162
XXVI.	Fe-Plated Platinum Working Electrode	163
XXVII.	Product Distribution for SEM Examined Electrodes	169
XXVIII.	Integrated Areas Beneath Curve C for Preelectrolyzed Reactions of Iron Salts	181
XXIX.	Effects of Cumene on Product Production in Two-Electrode Cell at Constant Applied Potential, 1.5V	182
XXX.	Other Organic Substrates Examined with $Fe(acac)_3$ in Three-Electrode Cell	185

Table		Page
XXXI.	Current Maximum for Appropriately Sized Resistors Used at R_2	199
XXXII.	Alloy Composition for Aluminum and Stainless Steel (180,181)	204

LIST OF FIGURES

Figure		Page
1.	d-Energy Level Splitting for Preferred Geometries of Group VIII Transition Metals	6
2.	Organic Synthesis with $Na_2Fe(CO)_4$ (12,16,18)	11
3.	Thermal Decomposition Route for η-$C_5H_5Fe(CO)(P\emptyset_3)$(n-Bu) (55)	27
4.	Reactions of $FeEt_2(dipy)_2$ (57,58)	29
5.	Electrochemical Degradation of Organotransition Metals (90,93)	42
6.	Two-Electrode Electrolysis Cell	46
7.	Polarogram for Two Electrophores	47
8.	Macroscopic Cell with Two Solution Electrophores (101)	49
9.	Current-Time Curves for Two Systems with Different Electrochemical Rate Constants (68)	53
10.	Current-Time Behavior for Three Representative Two-Electrode Constant E_{APP} Electrolysis Cells with Aluminum Electrodes	58
11.	Cathode Potential versus Time for a Two-Electrode Constant E_{APP} Electrolysis. Potential Monitored with Cd(Hg) Reference	61
12.	Idealized Cyclic Reaction with Iron Mediator and Alkyl Halide	62
13.	Idealized Working Electrode Potential versus Total Cell Current for Solid State Potentiostat with Current Limiting Override	77

Figure		Page
14.	Cell Current versus Working Electrode Potential Curves for (I) 0.2M $Fe(acac)_3$ and (II) 0.8M $1\text{-}C_8H_{17}Br$ at an Aluminum Working Electrode	82
15.	Cell Current versus Time Behavior for a Three-Electrode Cell with $Fe(acac)_3$, $1\text{-}C_8H_{17}Br$, Aluminum Electrodes, and E_{ref} = -0.90V vs Cd(Hg)	83
16.	Separability of Current Transcients	85
17.	Cell Current versus Time Behavior for $FeBr_3$	87
18.	Exploded View of Aluminum Working Electrode Illustrating Possible Galvanic Cell Between Al(0) and Fe(ions)	91
19.	Cell Current versus Working Electrode for $Fe(acac)_3$ at Aluminum, A, and Stainless Steel, B, Electrodes in Macro-electrolysis Cell	95
20.	Cell Current versus Time Behavior of $Fe(acac)_3$ at a Stainless Steel Working Electrode	99
21.	Cell Current versus Time Behavior for Blank Reaction NII178	111
22.	Three-Electrode Alignment with Pt Counter Electrode . . .	126
23.	Cell Current versus Working Electrode Potential for Different Aluminum Pretreatments	131
24.	Cell Current versus Time Behavior for Reduction of $Fe(acac)_3$ at Various Pretreated Aluminum Working Electrodes	133
25.	Absorbance Spectra Before (I) and After (II) Electrolysis of $Fe(acac)_3$ with $1\text{-}C_8H_{17}Br$ at Aluminum Electrodes in Two-Electrode Constant Applied Potential Electrolysis Cell	149

Figure		Page
26.	Absorbance Spectrum for Reaction NII146	153
27.	Absorbance Spectra for Reduction of $Fe(acac)_3$ with Mixed Electrode Systems	155
28.	Absorbance Spectra of (I) An Electrolyzed $Fe(acac)_3$ Solution and (II) an Iron-Free Solution after Electrolysis Using an Fe-Plated Aluminum Electrode, Working Electrode, and an Aluminum Counter Electrode	156
29.	Scanning Electron Micrograph of the Iron-Plated Aluminum Working Electrode for Reaction NII184	166
30.	Scanning Electron Micrograph of the Iron-Plated Aluminum Working Electrode for Reaction NII188	168
31.	Formation of Products versus Time	175
32.	Geer's In-House Manufactured Potentiostat	198

ABSTRACT

The electrochemical reduction of an N,N'-dimethylformamide, DMF, solution of iron (III) acetylacetonate, $Fe(acac)_3$, in the presence of 1-octyl bromide has been investigated. The strategy for the reaction is to selectively reduce the metal ion to a lower valent state without concomitant electrochemical reduction of the organic halide. The 1-octyl bromide was converted to octane, 1-octene, and hexadecane.

Electrolysis cells were operated with either a constant applied potential across two aluminum electrodes or with potentiostatic control of the working electrode potential. The latter cell required the generation of a stable reference electrode suitable for use in DMF. The cadmium amalgam reference electrode was such a reference. The yields of hexadecane ranged from 0 to 33% for identically assembled two-electrode cells operating with a 1.5 volts applied across two aluminum electrodes. Potentiostatic control of the working electrode potential was hoped to decrease the wide range in yields of coupled product, however, this did not occur. Using an aluminum working electrode in identically assembled three-electrode electrolysis cells operating with the working electrode potential held at -0.9V vs Cd(Hg), the yields of hexadecane ranged from 35 to 59%.

The current-time behavior for the reduction of $Fe(acac)_3$ in the presence of 1-octyl bromide using aluminum electrodes was recorded for both the two-electrode and three-electrode electrolysis cells. The current increased steadily with time for the two-electrode cell run at constant applied potential before falling to near zero levels. This is unusual for a simple reduction. The three-electrode cell held at a constant working electrode potential of -0.9V vs Cd(Hg) generated two current transients. The first current transient was generated as a result of iron plating onto the aluminum working electrode. The overpotential for reducing iron ions at an iron surface is less than the overpotential for the same reduction at aluminum, therefore the increase in current. The second current transient is assigned to the formation of an organoiron which is also electroactive.

The conversion of 1-octyl bromide to hexadecane, octane, and 1-octene is a one-electron heterogeneous reaction occurring at an iron-plated surface. The 1-octyl bromide is suggested to oxidatively add or dissociatively adsorb onto the active iron surface. A one-electron transfer occurs expelling a bromide ion. This corresponds to the second current transient. Products are formed as a result of free radical reactions. The reaction is sensitive to the pretreatment of

the aluminum electrodes, total cell current, and the nature of the plated iron surface. An epitaxial effect by the aluminum electrode is suggested to account for these observations.

INTRODUCTION

Transition metals and main group metals have become common reagents in organic synthesis. Stoichiometric or catalytic quantities of the metal are used independently or in concert with other metals for both homogeneous and heterogeneous transformations of the organic substrates to products. Early attention was given to the main group metals but a growing body of literature has begun to explore the organo-coordination chemistry of the transition metals. The wealth of information that is now being accumulated on organotransition metal complexes is a consequence of the interesting chemistry of these metals due to the availability of the d-orbitals of the metal and the realization that organotransition metal complexes are not inherently thermally unstable. The carbon-metal σ-bond in these complexes is probably no weaker than bonds between carbon and other non-transition metal elements (1-4). The previously implied thermal instability simply reflects the plethora of decomposition pathways available for these organotransition metal complexes (2-6). The existence of these routes of decomposition is of eminent importance in the use of the organotransition metal complexes for organic synthesis. The following sections are offered to acquaint the reader with some general aspects of Group VIII transition metal chemistry, specific homogeneous organic chemistry of iron, and electrochemical processes of organic halides and organotransition metal complexes. These areas of the

literature have culminated in this examination of iron and alkyl halide reactions in an electrochemical cell.

General Group VIII Transition Metal Chemistry

The group VIII transition metals, of which iron is a member, participate in a wide variety of homogeneous reactions (7,8). Even a cursory examination of the group VIII transition metal chemistry requires several considerations to be put forth at the onset. First, the oxidation number of the central metal in the complex is defined as the charge left on the metal after all the ligands are removed in their closed-shell configuration (7,8). Thus, an alkyl radical is a one electron donor, but in computing the oxidation number of the metal, this group is considered a carbanion. A coordinated olefin is a two electron donor and, in computing the metal's oxidation number, it is removed as a two-electron ligand, therefore no change in the oxidation number of the metal occurs. Table I gives a brief classification of the number of electrons some commonly coordinated ligands donate to the metal. Second, the d-electron configuration about the central metal of the complex is assigned as a low-spin metal center with the d-orbitals split by the appropriate ligand field. The electrons fill the lowest energy d-orbitals with pairing, if necessary, before filling higher energy levels. Nonbonding and slightly π-bonding orbitals are filled before the antibonding orbitals. Finally, the 18-electron

Table I. Classification of Ligands on the Basis of Donated Electrons (8)

Number of Electrons Donated	Compound or Ligand
1	R•, aryl, H•, X•, CN•
2	CO, PL_3, ethylene, NH_3 L = aryl, alkyl, etc.
3	π-allyl•, NO (nitrosyl)
4	diene, triene, etc., but only two double bonds are coordinated
5	cyclopentadienyl
6	benzene, cycloheptatriene

rule, which is an empirical statement of the tendency of the transition metal center to acquire the next inert gas configuration, is usually obeyed by the group VIII metals although 16-electron square planar complexes for these metals are not unusual. Tolman (9) has noted a relationship between the 16- and 18-electron configuration about the central metal and the tendency for these complexes to participate in homogeneous catalytic cycles.

The normal range of the d^n electron configurations for the group VIII transition metals is from d^6 to d^{10} with a d^8 configuration being particularly widespread. Collman (8) has partitioned the even d^n configurations and coordination numbers of various possible complexes into saturated and unsaturated systems.

d^n	Saturated	Unsaturated
d^6	6 ligands	5 ligands
d^8	5 ligands	4 ligands
d^{10}	4 ligands	3 or 2 ligands

The utility of this classification lies in the experimental observation that coordinatively unsaturated systems are chemically active. Therefore, reasonable induction times are normally required to activate the saturated complexes (9).

Halpern (7) has further elaborated on this attempt of classification. He has examined the reactivity patterns of these transition

metals and compared the metal complexes to analogous intermediates in organic chemistry. Table II compares such a classification of the transition metals with organic intermediates. Appropriate examples are provided to accentuate the similarities.

The utility of this classification is best demonstrated with an example. The types of reactions associated with a particular electronic configuration and coordination geometry about the metal center can be related using the ligand field split d-orbitals of the preferred geometries of group VIII metals as shown in Figure 1. Consider the nature of the reaction in which an electron is added to an octahedral d^6 complex. The electron goes into an antibonding orbital of the octahedral complex. This is destabilizing. The detrimental effect can be relaxed if the system transforms into another geometry such as trigonal bipyramidal by loosing a coordinated ligand. This process, as pointed out by Halpern (7), is analogous to that which occurs when an electron is added to a saturated carbon compound:

$$\underset{\text{very stable}}{CH_3X} \xrightarrow{+e^-} \underset{\text{unstable}}{[CH_3X]^-} \rightarrow \underset{\text{stable}}{CH_3\cdot} + X^- \qquad (1)$$

$$\underset{d^6}{Co(CN)_6^{3-}} \xrightarrow{+e^-} \underset{d^7}{(Co(CN)_6^{4-}]} \rightarrow \underset{d^7}{Co(CN)_5^{3-}} + CN^- \qquad (2)$$

Extending this analogy to the systems in Table II while using the

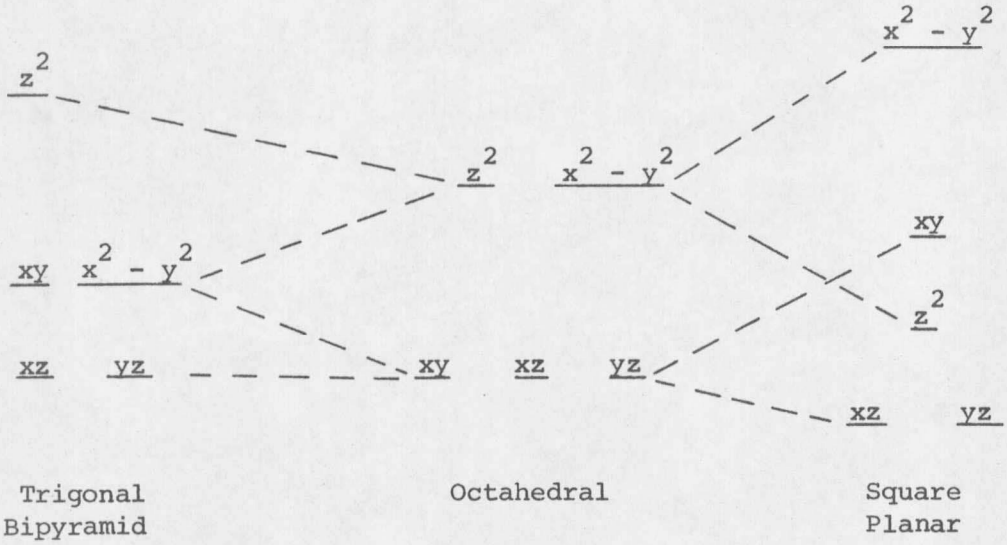

Figure 1. d-Energy Level Splitting for Preferred Geometries of Group VIII Transition Metals.

Table II. Comparison of Coordination Chemistry and Organic Chemistry Intermediates (7)

Species	Coordination Number	Nonbonding Electrons	Characteristic Reactions	Coordination Number	Nonbonding Electrons	Examples	Reactions
Saturated Molecule ($R_3C - X$)	4	0	Substitution	6	6	$RhCl_6^{3-}$	$RhCl_6^{3-} + H_2 \rightleftarrows RhCl_5H^{3-} + HCl$
Free radical ($R_3C\cdot$)	3	1	Dimerization	5	7	$Co(CN)_5^{3-}$	$2Co(CN)_5^{3-} \rightleftarrows Co_2(CN)_{10}^{6-}$
			Abstraction				$Co(CH)_5^{3-} + CH_3I \rightarrow Co(CH)_5I^{3-} + CH_3\cdot$
			Addition				$2Co(CH)_5^{3-} + HC{\equiv}CH \rightarrow$ $(NC)_5CoCH{=}CHCo(CH)_5^{6-}$
Carbene $R_2C{:}$	2	2	Addition	4	8	$IrI(CO)(PPh_3)_2$	$IrI(CO)(PPh_3)_2 + C_2H_4 \rightleftarrows$ $IrI(CO)(C_2H_4)(PPh_3)_2$
			Insertion				$IrI(CO)(PPh_3)_2 + H_2 \rightleftarrows$ $IrH_2I(CO)(PPh_3)_2$
Carbonium ion (R_3C^+)	3	0	Addition of nucleophile	5	6	$Co(CN)_5^{2-}$	$Co(CN)_5^{2-} + I^- \rightleftarrows Co(CN)_5I^{3-}$
Carbanion ($R_3C{:}^-$)	3	2	Addition of electrophile	5	8	$Mn(CO)_5^{1-}$	$Mn(CO)_5^- + H^+ \rightleftarrows Mn(CO)_5H$

concepts of the unsaturated and saturated classification of Collman (8), the following generalized system of reactions can be developed:

d^6(5CN)*	$\xrightarrow{+L}$	d^6(6CN)	carbonium ion
d^7(5CN)	$\xrightarrow[+L]{-e^-}$	d^6(6CN)	free radical
d^8(4CN)	$\xrightarrow[+2L]{-2e^-}$	d^6(6CN)	carbene (oxidative-addition)
d^8(4CN)	$\xrightarrow{X}$	d^8(5CN)	carbene (X = CO or olefin)
d^8(5CN)	$\xrightarrow[+L]{-2e^-}$	d^6(6CN)	carbanion

*(coordination number)

In this scheme, L is any ligand and the number in parenthesis is the coordination number of the central metal. The importance of this type of classification is obvious; the reactivity patterns of the central metal depend on both its electronic configuration and the geometry, i.e., coordination number, of the complex. From such a classification, the oxidative-addition reaction which is widespread in the homogeneous reactions of the d^8 unsaturated square planar complexes of the group VIII transition metals arises from a concerted insertion of the d^8 complex into an X-Y bond. In so doing, the electron configuration and the coordination number about the metal center have changed by two. The existence of this reaction pathway is important in organotransition

metal chemistry in that it is often suggested to be a component of a homogeneous catalytic cycle. The propensity for undergoing the oxidative addition reaction increases upon descending a triad and passing from right to left (8). A word of caution should be injected at this juncture. The reaction scheme seems to suggest an inherent reactivity of saturated penta coordinated d^8 complexes. The trend for d^8 complexes to become coordinatively saturated (penta coordinated) increases on ascending the triad and going from right to left (8). Thus, the stability to CO dissociation for $M(CO)_5$ complexes is Fe > Ru > Os. Part of this stabilization is the availability of four π-backbonding orbitals in the trigonal bipyramid versus only three such orbitals in the square planar geometry (8,10).

The many pathways of decomposition that are available to the organotransition metal complexes have been reviewed elsewhere (5,6,11). Two decomposition pathways are of interest to this project. Reductive elimination reactions are essentially the reverse of oxidative addition reactions. The reaction involves a loss of two σ-bonded ligands together as a molecule. The coordination number and the oxidation state of the central metal decrease by two. β-hydride elimination occurs for alkyl transition metal complexes in which the alkyl group has hydrogens beta to the metal. This reaction requires a coordinately unsaturated site on the central metal. The beta hydrogen migrates to this site of coordinative unsaturation resulting in the formation

of an olefin-metal hydride complex. The olefin can then dissociate from the metal-hydride. The general sequence of events is depicted in the following equation:

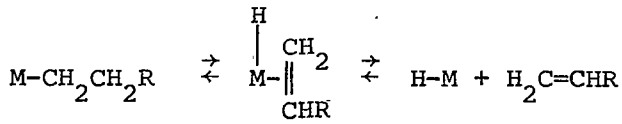

Iron Chemistry

The general chemistry of the group VIII transition metals is typified by the reactions of iron in various oxidation states. Five oxidation states are available to the iron and have been reported in the literature in various synthetic processes. These oxidation states are the -II which is not common but is found in the disodium tetracarbonyferrate salt, the zero, and the +I, +II, and +III states.

The disodium tetracarbonylferrate salt, $Na_2Fe(CO)_4$, has been suggested to be the transition metal analog of a Grignard reagent (12). The work of Collman et al. (13-15) has established the versatility of this reagent in synthetic organic chemistry. Two excellent reviews discuss the wide utility of this reagent from which Figure 2 has been abstracted (12,16). The reagent is useful in preparing aldehydes, unsymmetrical ketones, carboxylic acids, esters, and amides. The very high electron density on the iron (d^{10} configuration) makes the iron a particularly potent nucleophile (17). The reaction could proceed by either an S_N2 attack on the alkyl halide with inversion of

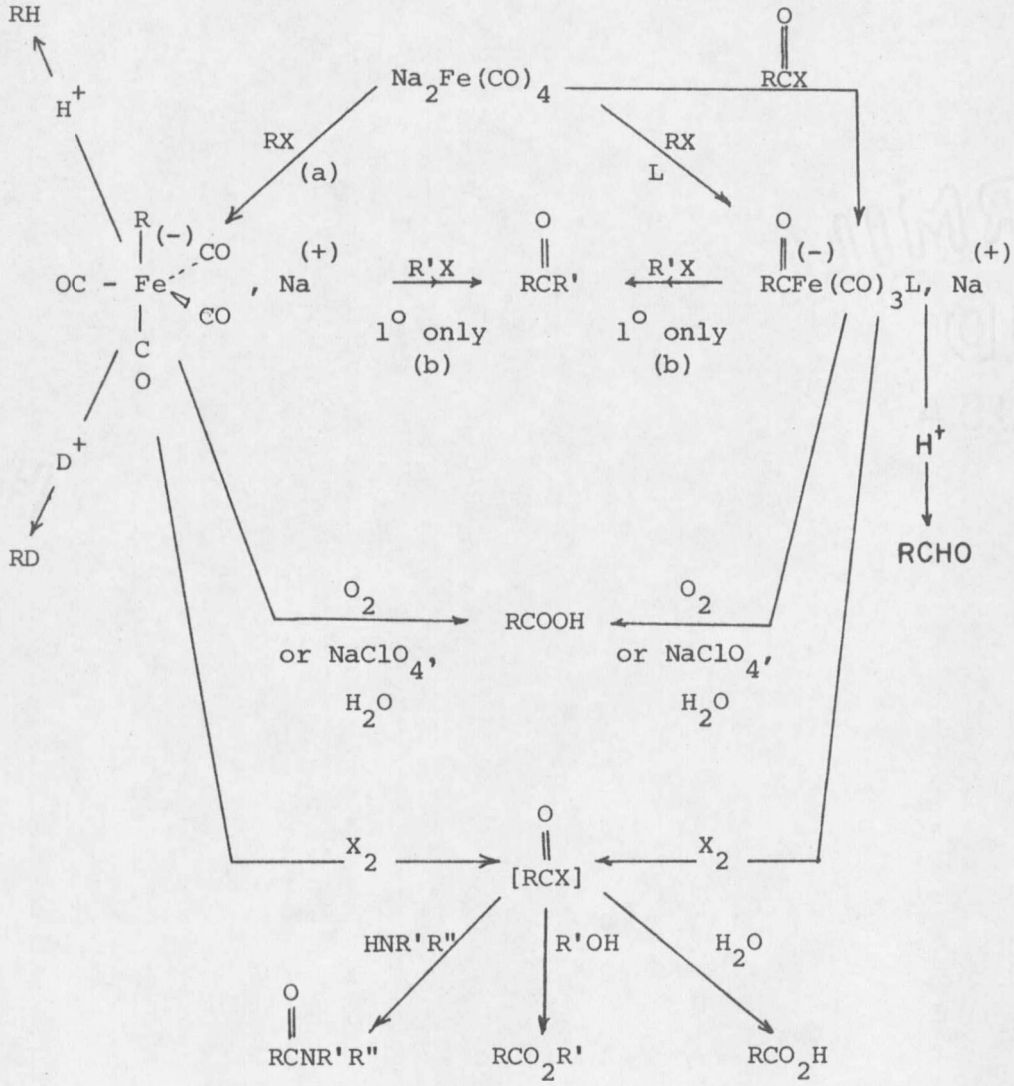

Figure 2. Organic Synthesis with $Na_2Fe(CO)_4$ (12,16,18).

configuration, or by oxidative addition to a d^{10} iron (-II)(13) defined to reflect the addition of a covalent molecule to the coordination sphere with reduction in the oxidation number of the metal (8). Both pathways would reduce the electron density about the iron center. Step (a) of the reaction sequence was observed to proceed with primary bromides, iodides, and tosylates as alkylating agents. The second alkylation, step (b), required more reactive reagents such as primary iodides or tosylates or benzylic halides. The overall order of reactivity for various reagents in the first step is ROTs $\sim$ RI > RBr > RCl and 1° > 2° > 3°; in fact, the tertiary halide failed to react. This order of reactivity and the noted inversion about the carbon center was used to argue for a classical S_N2 alkylating step corresponding to the formation of the alkylated iron species. Subsequent formation of the acyl group proceeds with retention of configuration by migratory insertion of the carbonyl ligand into the alkyl metal bond (12).

The advantages which this complex has over the classical Grignard reaction are generally high yields of products, stereospecificity, and the toleration of several functional groups within the substrate such as -CHO, $-CO_2R$, -C≡N, and -Cl. There are some limitations to its usefulness. The high electron density on the iron makes it a particularly effective base in promoting elimination reactions. Allylic halides are also not usable because of their propensity to form π-complexes with the tricarbonyl iron. Like the Grignard reagents, the

iron complex must be used in excess to be effective in maximum conversion of organic substrate to product. Finally, the carbonyl insertion step is so facile in this complex that dialkylated iron species do not form which, on decomposition, could lead to coupled product without a carbonyl carbon inserted.

Iron zero, Fe(0), is a d^8 metal. Reactions of iron in atomic or aggregate form have been observed in homogeneous and heterogeneous systems respectively. Suspensions of iron powder in water have been noted to couple benzyl chloride (19) and α,α′-dichlorotoluene (20). Radicals are formed during this reaction. In the benzyl chloride case, these radicals were intercepted by anthracene which led to the generation of mixed organic products RR′. The proposed reaction for coupling was

$$PhCH_2Cl \underset{\Delta}{\overset{H_2O}{\rightleftharpoons}} PhCH_2^{(+)} + Cl^{(-)}$$

$$2PhCH_2^{(+)} + Fe^{\circ} \rightarrow 2PhCH_2^{\bullet} + Fe(II)$$

$$2PhCH_2^{\bullet} \rightarrow PhCH_2CH_2Ph$$

The oxidation state of iron changes to +II during the reaction which corresponds to a $d^8 \rightarrow d^6$ transition. Although the yields of bibenzyl were not reported, the formation of benzal chloride from

α,α'-dichlorotoluene was 9.6%. The coupling which does occur does not lead to a substantial generation of products.

The vapor phase reaction of iron atoms with organic substrates has also been examined. The method involves the vaporization of iron powder in a vacuum chamber and cocondensation of the gas-phase iron with organic substrate. The usual organic substrate was an unsaturated hydrocarbon. In one system, acetylene was observed to adsorb very rapidly onto the iron (21). Dienes were also found to form complexes with iron zero and, in the case of 1,3-cyclohexadiene, proceeded on to generate products (22): cyclohexene (33.4%), benzene (36.4%), and 1,4-cyclohexadiene (30.2%). This complex formation is reasonable. Olefins are particularly good coordinators to iron zero since π-backbonding through the olefin π^* orbital is a reasonable route in reducing the electron density about the iron zero.

Iron carbonyls are perhaps the best known iron (0) compounds. Several iron carbonyl complexes form: $Fe(CO)_5$, $Fe_2(CO)_9$, and $Fe_3(CO)_{12}$. The latter two represent cluster type compounds with bridging carbonyl ligands. The pentacoordinated iron (0) exists as a trigonal bipyramid and, as stated earlier, represents the most stable conformation of this d^8 metal complex. Any reaction that this species can undergo requires the initial removal of a CO ligand using either photochemical or thermal stimulation in order to obtain a coordinatively unsaturated 16-electron system (9). After such activation, the

tetracarbonyl iron (0) can react in one of two ways. The intermediate can coordinate an olefin which, like CO, is capable of π-backbonding. This type of substitution reaction would be classified a carbene-like reaction (7). Alternatively, the metal complex can undergo oxidative addition which is another carbene-like reaction in which the metal complex inserts into an activated C-X bond. Several examples of these reactions are presented.

Alper et al. (23) has reported that the iron pentacarbonyl complex will react with 1°, 2°, and 3° aryl and alkyl α-haloketones in boiling 1,2-dimethoxyethane to give the coupled 1,4-diketone, reduced monoketone, and occasionally β-epoxyketones. They also noted that the iron pentacarbonyl will not react with the simple unactivated monohalides although the complex does react with activated geminal dihalides and vicinal dihalides. The reaction was not catalytic nor was it affected by free radical scavengers.

The reaction of a tetracarbonyl iron (0) complex with an olefin leads to the formation of cyclopentanones via a carbonyl insertion step. Weissberger et al. (24,25) photolyzed a sample of the pentacarbonyl iron (0) to generate the $Fe(CO)_4$ which subsequently coordinated an olefin. A reversible loss of another CO ligand from the monoolefin tetracarbonyl iron (0) complex allowed for further coordination of a second olefin. A five-membered metallocycle was formed from the coordinated olefins and metal center. A coordinated carbonyl group

inserts into one of the metal-carbon bonds thus forming a complex with a carbon-metal σ-bond and an acyl carbon-metal bond. Extrusion of the metal results in the formation of a cyclopentanone group linking the two olefins

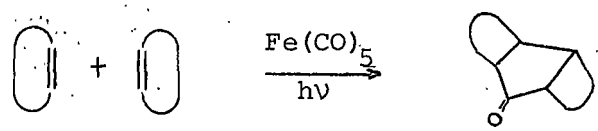

The formation of the products was stereospecific--exo-trans-exo was formed exclusively when substituted norbornene systems were used. This stereoselectivity has been suggested to be a consequence of the olefin π* acceptor orbital (26).

Mono coordinated olefins of the tetracarbonyl iron (0) complex can be treated with acid, HCl or HBr, to generate an iron (II)-alkyl intermediate. The intermediate then decomposes to alkane and an Fe(II) complex (27).

The ease of carbonyl insertion into a coordinated carbon-metal bond provides a route to possible ring expansion for appropriate systems. Weissberger (28) has observed the stereospecific expansion of pinene induced by iron pentacarbonyl to give the indicated products

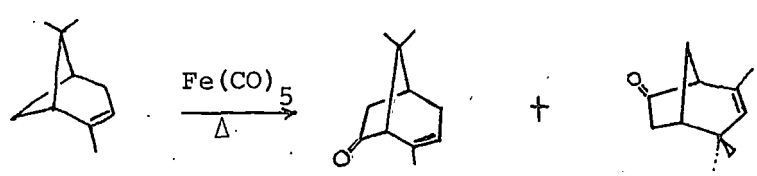

The reaction is felt to proceed via a σ-π-allyl metal complex and an acyl-π-allyl intermediate. Other ligands are capable of quenching the

reactive intermediate formed during the loss of a coordinated ligand. One such ligand is Ph_3P which is reported to be as effective in scavenging the iron (0) complex as is the olefin (29,30).

π-allyl metal derivatives of several metals have been recently reviewed (31). The π-allyl group is a three electron donor in π-complexes (8). It can coordinate with a metal as a σ-carbon species 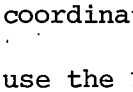 M or as an allyl group -M. These possible bonding combinations are designated η^1- and η^3-allyl respectively. This allows for some very interesting chemistry. The reactive transition metal salts are coordinatively unsaturated. In the above case, it may be possible to use the η^3-allyl system to protect a site of unsaturation which is then exposed to an appropriate substrate during the transformation of the η^3-allyl group to an η^1-allyl system. Thus, depending upon the nature of the added ligand, the equilibrium between the σ-bonded and π-bonded allylic iron can shift. Cardaci et al. (32) observed that donor ligands caused the system to shift to σ-bonded carbon-metal bonds while acceptor ligands favored the π-allyl configuration.

The particular degree of complexation for polyolefins depends on the availability of good coordinating ligands which, as in the π-allyl case, can shift the nature of the bonding. A series of possible η^2-(monoolefin) to η^4-(diolefin)-1,4-diene complexes of iron (0) have been used to examine the consequences of the Woodward-Hoffman formalism as it applies to transition metal chemistry (33). Hughes et al.

(34) have demonstrated that the thermally disallowed 1,3-hydrogen suprafacial shifts which Mango postulates to occur in the presence of transition metals does not occur with the iron complex. They also observed direct metal insertion into a C-H bond and direct hydride transfer.

The above presentation has elaborated on systems of iron (0) in which a π acid has been coordinated to the zero valent iron. These π acids have been typed as such because of their ability to form π-back bonds. Can a stable σ-alkyl-iron zero compound form? A recent report has established the crystal and molecular structure of an iron zero-carbanionic salt (35). The salt, $[(\{C_6H_5\}_3P)_2N][Fe(CO)_4C_3H_7]$ contained a carbanionic propyl group attached to iron. This complex is very interesting in that the propyl group is formally a two electron donor without any ability to π-back bond. Since this complexing increases the electron density on the metal center, the existence of such a complex would not have been predicted on the basis of the pedestrian arguments posed here. The coordination about the anionic iron center was reported to be trigonal bipyramidal.

The cyclopentadienyl ligand stabilizes the low valent iron zero in the sodium salt, $Na[\eta^5\text{-}C_5H_5Fe(CO)_2]$. Again, the iron is the central metal of an anionic fragment. This complex is particularly suited to nucleophilic attack on the alkyl halides due to the electron density on the metal. Nucleophilic attack would generate a σ-bonded alkyl metal

derivative of iron (II). The attack by this nucleophilic complex is classified as a carbanion attack on an electropositive carbon (36).

$$\underset{d^8}{Na[\eta^5\text{-}C_5H_5Fe(CO)_2]} + RX \rightarrow \underset{d^6}{\eta^5\text{-}C_5H_5FeR(CO)_2} \quad \xrightarrow[+L]{-2e^-}$$

This synthetic route has been used to prepare several σ-bonded alkyl-iron (II) complexes (37) including an optically pure chiral iron complex (38).

A very interesting reaction which is catalytic with respect to the reduced form of iron in the system is the Kharasch reaction (39,40) in which an organic Grignard reagent is mixed with a catalytic amount of ferric chloride in the presence of an organic halide.

$$RMgX + R'X \xrightarrow{FeCl_3} [RH, R(-H), R'H, R'(-H), RR, R'-R', RR']$$

The products of this reaction are monomeric alkanes and olefins (RH, R(-H), etc.) as well as coupled products (RR, etc.). The mechanism of this reaction has been extensively studied by Kochi et al. (41-46) and is suggested to be

$$RX + Fe \rightarrow R\bullet + FeX \qquad \text{(oxidation)}$$

$$R\bullet + Fe \rightarrow RFe \qquad \text{(oxidation)}$$

$$R'MgX + FeX \rightarrow R'Fe + MgX_2 \qquad \text{(metathesis)}$$

$$R'Fe, RFe \rightarrow \text{products} \qquad \text{(reduction)}$$

The reduced form of iron in this system has been shown to be the d^7 iron (I) species generated by a metathesis reaction between the Grignard reagent and the iron (III or II) of the added salt (44). The reduction of the iron involves an alkyl iron (III) species which proceeds through several steps before forming iron (I). An example of this reduction is given for an ethyl Grignard and $FeCl_3$.

$$Fe(III)Cl_3 + CH_3CH_2MgBr \rightarrow CH_3CH_3Fe(III)Cl_2 + MgClBr$$

$$CH_3CH_2Fe(III)Cl_2 \rightarrow \begin{array}{c} CH_2 \quad H \\ \| \quad | \\ CH_2 \quad Fe(III)Cl_2 \end{array} \rightarrow \begin{array}{c} CH_2 \\ \| \\ CH_2 \end{array} + Fe(III)HCl_2$$

$$CH_3CH_2Fe(III)Cl_2 + Fe(III)HCl_2 \rightarrow CH_3CH_3 + 2Fe(II)Cl_2$$

$$Fe(II)Cl_2 + CH_3CH_2MgBr \xrightarrow{O} Fe(I), \text{ etc.}$$

The absence of butane in the reduction of the iron (III) eliminates any free radical component since six times more butane than ethane should have formed (44). The iron complex Kochi used in this analysis to generate the iron (I) center was iron (III) acetylacetonate, $Fe(acac)_3$.

The coupling reaction which leads to the dimeric product is sensitive to the number of available beta hydrogens on the organic substrate. As noted above, the reduction of iron (III) ion by the Grignard reagent proceeds in several steps, one of which includes

β-hydride migration. The availability of beta hydrogen on the organic halide substrate would also provide a low energy path of decomposition for the organoiron complexes formed from this material thus reducing or eliminating any coupling reaction. As an example, ethyl bromide, ethyl Grignard, and ferric chloride produced a 1:1 ratio of alkane to alkene with less than 0.1% n-butane (42). When t-butyl bromide was used in place of ethyl bromide, iso-butane and iso-butene were formed with ethane and ethylene. No products from the t-butyl bromide were obtained when styrene was present indicating a free radical component of the overall mechanism.

The generation of alkane and alkene was felt not to occur by a free radical reaction involving the homolysis of an iron-alkyl bond since no coupled product was obtained. Either a two step hydride migration or a direct hydride migration via a bimolecular reaction of two alkyl-metal complexes was suggested to generate alkane and alkene.

$$\text{2-step} \quad RCH_2CH_2M \rightleftarrows RCH{=}CH_2 + HM$$

$$HM + RCH_2CH_2M \rightarrow RCH_2CH_3 + 2M$$

$$\text{direct} \quad 2RCH_2CH_2M \rightarrow RCH{=}CH_2 + RCH_2CH_3 + 2M$$

Coupling was suggested to proceed via a bimolecular reaction of two alkyl-metal complexes. Substrates without beta hydrogens coupled readily because the facile β-hydride migration decomposition

route was blocked. Added Ph_3P also increased the yield of coupled product for those systems without beta hydrogen (41).

The mechanism of the Kharasch reaction can be compared with recent work reported on gas phase ion-molecule reactions between iron (I) and CD_3CH_2I (47). Iron was observed to insert into the carbon-halogen bond forming an alkyl metal halide moeity. Furthermore, the β-hydride shift was explicitly observed to occur (47) thus supporting the existence of this step in the Karasch reaction. Although this work was performed in the gas phase and the Kharasch reaction is run in a solvent (THF), there does appear to be a conflict between the carbene-like insertion (oxidative-addition) in the gas phase versus the free radical reaction between alkyl halide and iron (I) in the solvent. The gas phase work with methyl iodide gave nearly a 50/50 mixture of organic free radicals and iodine atoms. d_5-Ethyl iodide, on the other hand, generated only 14% ethyl radicals and 86% deuterium iodide leaving a stable coordinated olefin-iron complex. Thus, the gas phase reaction suggests that radical formation is not particularly facile compared to oxidative-addition/β-hydride migration bringing into question the initial step of the Kharasch reaction, free radical generation.

Reactivity patterns of the Grignard reagent have established the pattern Et > n-Pr > i-Pr > neopentyl > CH_3 > ϕCH_2 > C_6H_5. Similarly,

the reactivities of the alkyl bromides have demonstrated the following order of decreasing reactivity: t-Bu > i-Pr > n-Pr (43).

Vinyl bromides were also observed to be reactive in the Kharasch reaction (42,45,46). This coupling reaction was observed to be stero-selective for products were cis or trans depending on the conformation of the vinyl moiety. The reaction is thought to proceed via coordination of the olefinic double bond to iron (I) with subsequent activation of the coordinated complex to halogen abstraction.

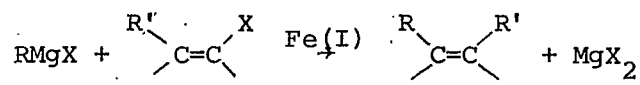

The stereospecificity of the reaction is suggested to reflect a concerted process in which a reduced iron species, Fe(I), is again the active agent.

$$Fe(I) + R'Br \rightleftarrows Fe(R'Br)$$

$$Fe(R'Br) + RMgX \rightarrow RR' + MgXBr + Fe(I)$$

This mechanism differs from the alkyl halide case in that no homolysis of the alkyl halide bond occurs. The mechanism is consistent with the coordinating abilities of the olefin. The coordination of the olefin allows for sterochemical specificity if the metathesis reaction between the Grignard and the olefin-iron complex results in the coordination of the Grignard's alkyl moeity on the iron center.

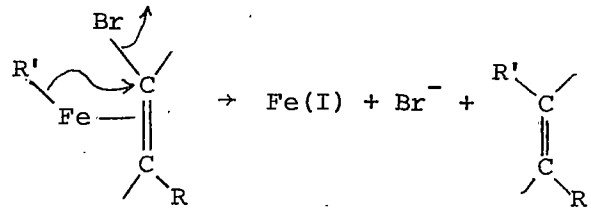

Recently Smith and Kochi (46) have suggested that the process involves oxidative addition of the vinyl bromide to the reduced iron with retention of configuration. They postulated the catalytic cycle

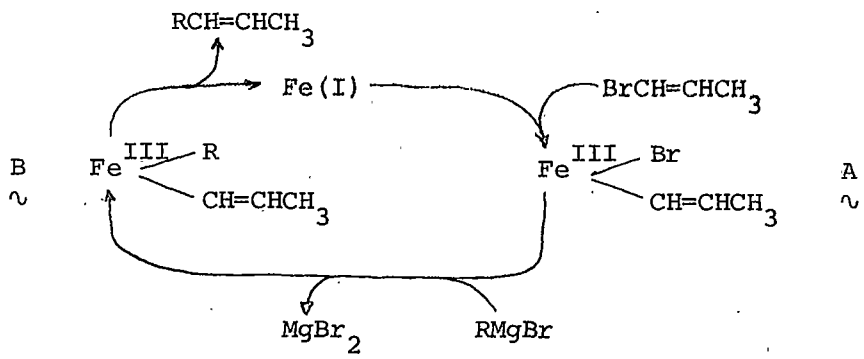

The catalytic effects of small amounts of iron (III), $\sim 10^{-5}$, in the Kharasch reaction has been observed for nearly sixteen years. It is interesting to read reports of peculiar effects that different sources of magnesium have on typical Grignard reactions (48,49). Examination of the magnesium from different sources found that the concentration of various transition metals varied with the source of magnesium. In particular, the effect of traces of iron impurities was monitored in the range of 4 to 40,000 ppm (48). Iron increased the yield of coupled product.

Iron (II) is a d^6 metal ion forming either octahedrally coordinated or tetrahedrally coordinated solution complexes depending on the particular ligand attached to the metal center. Iron (II)-alkyl metal complexes can be formed from the iron (0) anionic complex $Na[\eta^5\text{-}C_5H_5Fe(CO)_2]$ and alkyl halides generating the complex $\eta^5\text{-}C_5H_5Fe(CO)_2R$ which is thermally stable and insensitive to air oxidation in the solid state. Solutions of these complexes are air sensitive but, at room temperature, the complex is not labile. Whitesides et al. (50) have observed that the formation of the iron (II) complex proceeds with greater than 95% inversion of configuration at the carbon in the organic moeity. Generally, the reaction of low valent transition metals with alkyl halides can proceed with different stereochemical consequences depending on the method of reaction. If the metal acts as a nucleophile and displaces X^- from the organic substrate, the reaction is S_N2-like and proceeds with inversion of configuration (43). On the other hand, oxidative addition, particularly of d^8 complexes, proceeds with retention of configuration (43). Finally, ligand transfer of X^- to the metal reductant proceeds with racemization (43). The observation of 95% inversion substantiates the claim that the reaction is S_N2-like with the nucleophile being the iron (0) complex which has high electron density about the metal center. When the alkyl group is PhCHDCHD subsequent cleavage of the

alkyl-iron bond using Br_2, I_2, and $HgCl_2$ proceeds with retention of configuration of the alkyl ligand (51,52). If the alkyl group is $(CH_3)_3C$-, treatment of the complex with $HgCl_2$ cleaves the carbon-iron bond with retention of configuration (53,54) but Br_2 causes inversion at the carbon center (54).

Other reaction pathways are thermally accessible for this complex with R being the n-butyl moiety. Studies in hot solvent and in melts (55) have demonstrated that the thermal decomposition proceeds via β-hydride migration as demonstrated in Figure 3. Isolated products include the olefin and the metal hydride complex which was so stable, that it remained unreactive, therefore no saturated alkane was produced. Excess Ph_3P inhibited the formation of olefin by forcing the initial equilibrium to the left, therefore no sites of coordinative unsaturation were available for β-hydride migration. Recently, Norton (56) has suggested that hydride bridges between two metal centers are important in the elimination of alkane from a hydride and alkyl metal complexes. This suggestion appears to be in conflict with the noted generation of greater than 90% olefin from this iron (II) complex which generates both olefin and hydride. Since the olefin formation requires the generation of a coordinatively unsaturated site on the metal center, the availability of this vacant site for hydride bridging seems a reasonable pathway to initialize alkane production.

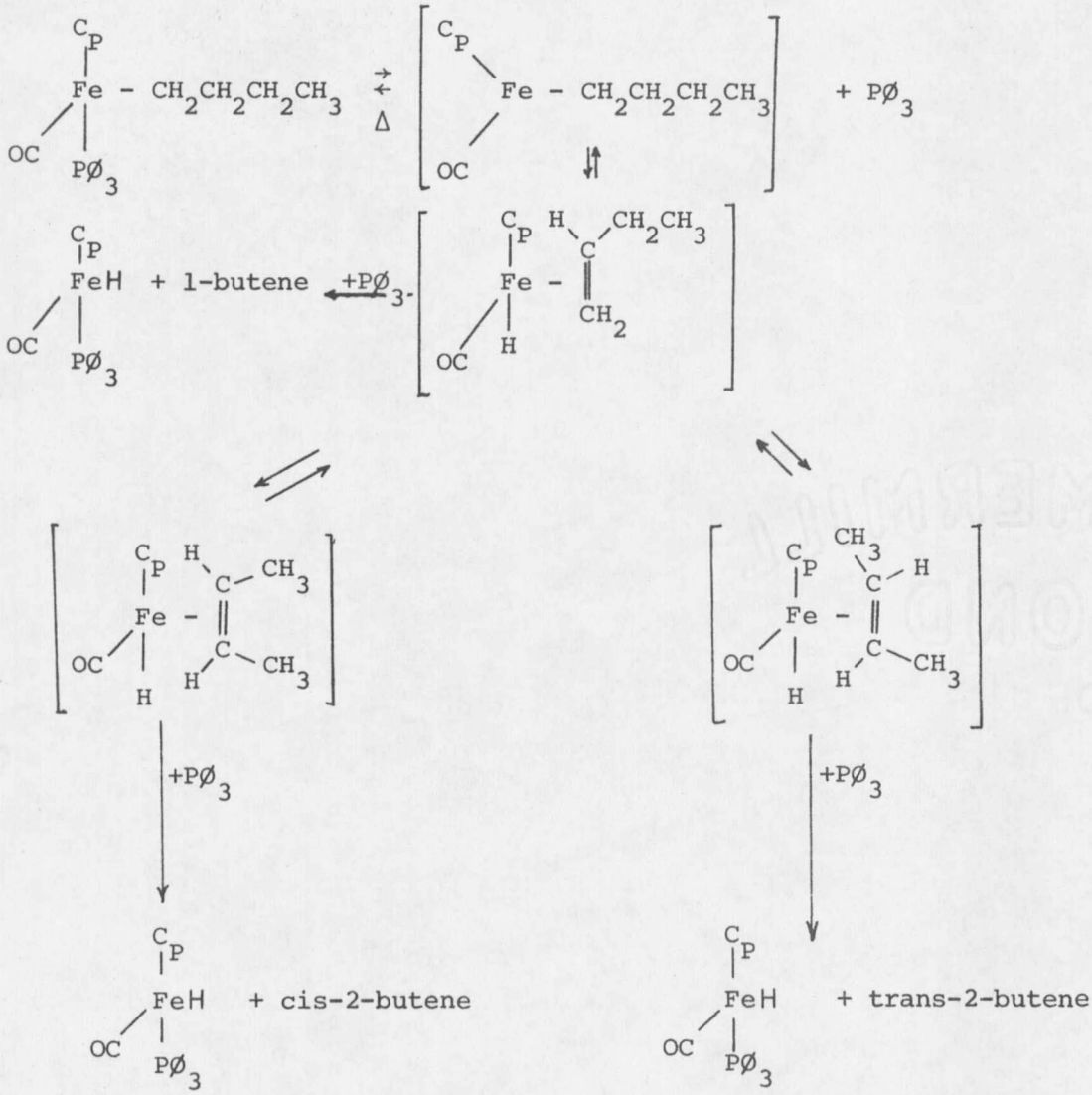

$P\emptyset_3$: triphenyl phosphine; C_P: η^5-cyclopentadienyl

Figure 3. Thermal Decomposition Route for η^5-$C_5H_5Fe(CO)(P\emptyset_3)(n\text{-}Bu)$ (55).

The work done on this bridging hypothesis involves osmium (II) which is also a d^6 metal in the same triad as iron.

Alkyl-iron (II) complexes have also been reported which are free of both the carbonyl and cyclopentadienyl ligands. Yamamoto et al. (57,58) have isolated diethylbis(dipyridyl)iron complexes from a catalyst system containing iron (III) acetylacetonate, diethyl aluminum monoethoxide, and dipyridyl. Iron (0), (II), and (III) complexes of the dipyridyl ligand were prepared by thermal degradation of the diethyl complex. The reaction scheme is given in Figure 4. Thermalosis is seen not to lead to any coupled product. Coupling can be initiated, but it is not the preferred route of decomposition. This diethyl complex was found to be an active catalyst in butadiene cyclodimerization. For this complex to function in such a process, the mechanism must involve the generation of a coordinatively unsaturated complex in order to allow for olefin coordination (58).

Iron (II) is also a good radical trap. The reaction of iron (II) with free radicals has demonstrated its versatility as a trap and a one-electron reductant (59-62). Functioning as a free radical trap, the iron (II) was observed to give coupled products from methyl free radicals via the proposed scheme (59):

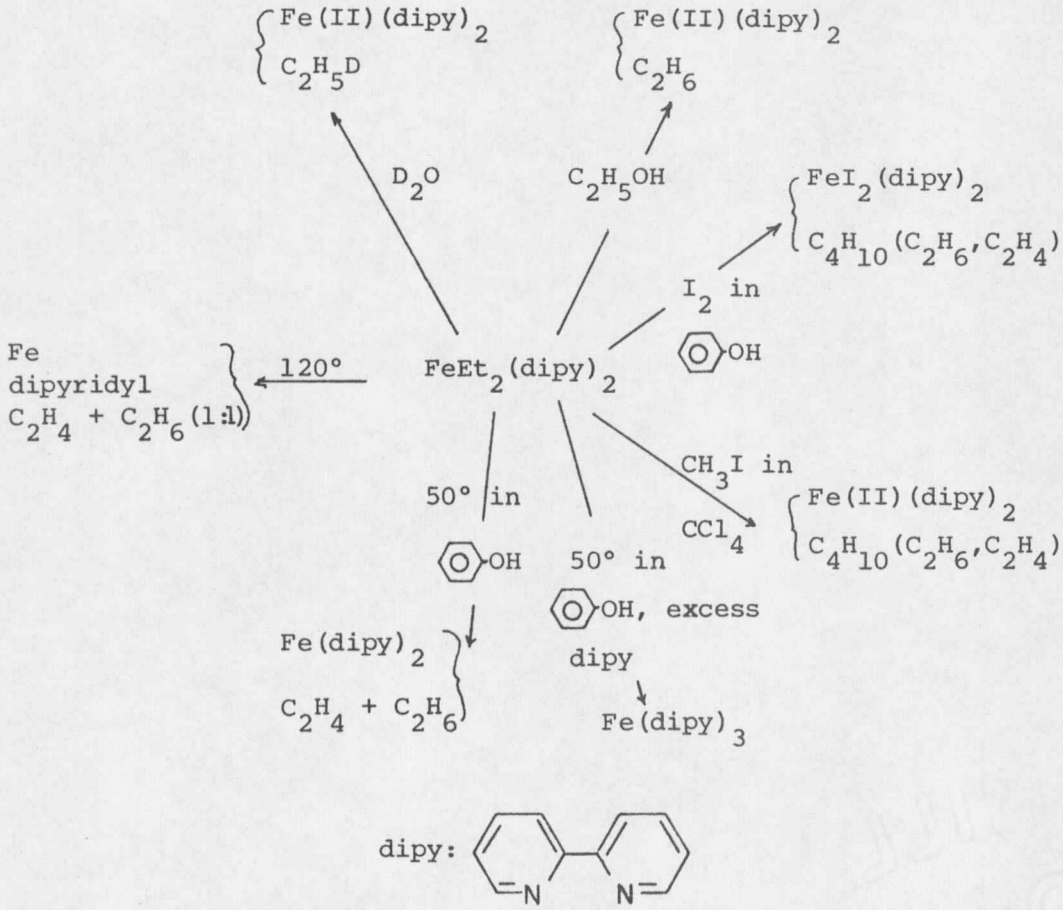

Figure 4. Reactions of $FeEt_2(dipy)_2$ (57,58).

$$R\bullet + M^{2+} \rightleftarrows (R\bullet M)^{2+}$$

$$R\bullet + (R\bullet M)^{2+} \rightarrow RR + M^{2+}$$

$$2(R\bullet M)^{2+} \rightarrow RR + 2M^{2+}$$

This reaction was particularly facile with Ni(II).

Iron (III) is the final oxidation state of iron that will be discussed. Iron (III) is a d^5 ion. The iron ion can effectively perform the functions of a free radical trap through its relative ease of reduction to iron (II). In particular, ferric chloride is a very effective trap for alkyl radicals, the product of the reaction being an alkyl chloride and ferrous chloride (63,64). The reaction is felt to proceed via a bridging chloride, i.e., an outer sphere reduction.

$$R\bullet + Fe(III)Cl_3 \rightarrow [R\bullet\bullet\bullet Cl\bullet\bullet\bullet Fe(III)Cl_2] \rightarrow RCl + Fe(II)Cl_2$$

The effect of free iron (III), that is without coordinated chloride, is to oxidize the free radical to the corresponding cation which proceeds to form products (65). The iron (III) ion is effective as a free radical trap, but of little utility in forming alkyl metal complexes, probably because of the low stability of an iron (IV) ion.

This discourse on iron organometallic chemistry suggests that the formation of the lower valent states of iron can lead to particularly effective reagents in organic synthesis. The oxidation states of iron (0) and iron (I) are noted to be more reactive than the

oxidation states (II) and (III) as demonstrated by both the iron carbonyl chemistry and the Kharasch reaction. The formation of these lower valent states has usually been accomplished with chemical reducing agents which have fixed but wide varying reduction potentials. This method of reduction generally limits the synthetic method in that the organic substrate is susceptible to reduction of unprotected functional groups. Secondly, the chemical reducing agent is usually required in excess concentrations to insure that all the iron remains reduced in which case a catalytic cycle is available. Alternatively, the iron is prereduced to a low oxidation state such as the iron in the disodium tetracarbonylferrate reagent. The reduced iron is susceptible to oxidation and therefore requires special handling. Another method of reduction uses an electrochemical cell to effect the reduction of an air stable iron salt in the presence of an organic substrate. The initial investigation into the utility of this method was done by Pillsbury (66). The method was successful. Electrochemical cells have also been used to form d^8 organometallic complexes from the d^6 organometallic parent (67). The synthesis outlined by Pillsbury is different in that the reduction, organometallic formation, and product generation are preformed in one cell without prior preparations.

Reduction of Organic Halides

The electrochemical reactivity of organic compounds has been thoroughly reviewed by Fry (68), Mann and Barnes (69), Baizier (70), and Rifi (71). The reaction of particular concern for this dissertation is the reductive cleavage of organic halides. The classical work of von Stackelberg and Stracke (72) established an electrochemical reactivity pattern for the organic halides that has recently been modified by Fry (68).

1. The ease of reduction of organic halides follows the order

allylic ≃ benzylic > saturated ≃ aryl > vinylic

Thus, allyl bromide has an $E_{1/2}$ = -1.29V(SCE), ethyl bromide has an $E_{1/2}$ = -2.09V(SCE), n-butyl bromide has an $E_{1/2}$ = -2.27V(SCE), and vinyl bromide has an $E_{1/2}$ = -2.47V(SCE). All of these reductions occurred in 75% dioxane-water solvent with tetraethylammonium bromide as the supporting electrolyte. SCE refers to the saturated calomel electrode used as a reference electrode.

2. The double bond in unsaturated halides is not electrochemically reducible.

3. The ease of reduction of a particular organic halide is a function of the attached halogen. The ease of reduction decreases (requires increasing cathodic potential) in the order

I > Br > Cl > F

In fact, except for unusual cases, the alkyl chlorides are not electrochemically reducible.

4. Geminal and vicinal polyhalides are easier to reduce than simple halides. This trend is adequately demonstrated in the following two series given in the order of decreasing ease of reduction:

$$CCl_4 > CHCl_3 > CH_2Cl_2 > CH_3Cl$$

$$BrCH_2CH_2Br > CH_3CHBr_2 > CH_3CH_2Br$$

5. An increase in chain length of the aliphatic group attached to a carbon atom reduces the ease of reduction:

methyl bromide > n-butyl bromide > n-octyl bromide

The nature of this effect has been attributed to adsorption phenomena.

6. In general, the half wave potentials for the reduction of organic halides are pH independent indicating that proton transfer to form the saturated system cannot occur either before or in the transition state of the reaction.

von Strackelberg and Stracke (72), on the basis of the above evidence, proposed the following mechanism for organic halide reduction:

$$RX + e^- \rightarrow R\bullet + X^-$$

$$R\bullet + e^- \rightarrow R^-$$

$$R^- + H^+ \rightarrow RH$$

Two other mechanisms have been suggested by Elving (73) one involving an S_N2 type reaction the other an S_N1 reaction:

$$S_N2 \quad RCH_2X + 2e^- \rightarrow RCH_2^- + X^-$$

or

$$RCH_2X + 1e^- \rightarrow [RCH_2X]^{\overset{\bullet}{-}}$$

$$[RCH_2X]^{\overset{\bullet}{-}} \rightarrow RCH_2^{\bullet} + X^-$$

$$RCH_2^{\bullet} + 1e^- \rightarrow RCH_2^-$$

$$S_N1 \quad RCH_2X \rightarrow RCH_2^+ + X^-$$

$$RCH_2^+ + 2e^- \rightarrow RCH_2^-$$

The latter mechanism was felt feasible by considering the effects of the intense electrical field within the electrical double layer. Petrovich and Baizer (74) have shown that the ease of reduction of alkyl halide followed the order of Br << OTs $\lesssim$ Cl. This order is inconsistent with an S_N1 displacement mechanism. Annino et al. (75) and Webb et al. (76) examined the reduction of optically active cyclopropyl halides and found partial retention of configuration. Again, the evidence was used to discount the S_N1 mechanism.

Lambert (77,78) and Marple (79) have been strong proponents of the S_N2 mechanism. They have demonstrated qualitative correlations between S_N2 reactivity and half-wave potentials. In this stead, the

cathode acts as an extremely large nucleophile. Ulery (80) indicated that two possible routes exist for this type of attack:

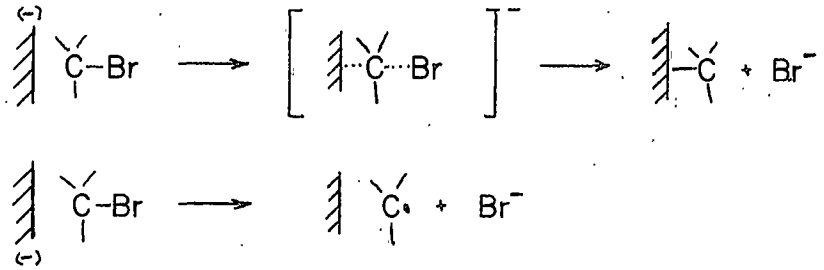

Sease (81) demonstrated that for bridge-head bromides, the S_N2 mechanism is not possible since backside attack is impossible. Noting that halogens can specifically adsorb on the surface of mercury, Sease considered the halogen functioning as a bridging group between the electrode surface and the alkyl group. In this configuration, an electron flows through the bromine atom from the cathode to the carbon. Lambert (82) argues against this mechanism and suggests that the orientation of the carbon-bromide dipole dictates that bromide cannot align itself with the cathode in this manner. He proposes either a perpendicular adsorption relative to the carbon-bromide bond axis or a possible S_N1 effect.

The intermediacy of the anion radical, $[R\text{-}X]^{\dot{-}}$, has been contested by Fry (68). The $[R\text{-}X]^{\dot{-}}$ may be a transition state but not a true intermediate. Studies of the reduction of alkyl halides by solvated electrons do involve intermediates with the structure $[RX]^{\dot{-}}$. This argues against their formation in an electrochemical

cell since the rates of reduction by hydrated electrons are unrelated to carbon-halogen bond strength while the electrochemical reductions do demonstrate such a relationship.

The first step of the reduction in the classical mechanism is felt to be rate limiting. Thus, the second electron transfer is very rapid and, if the first step of the reduction of the original halide occurs at potentials more cathodic than the reduction of the alkyl radical thus formed, a net two electron transfer occurs. The evidence for the intermediacy of free radicals comes from two sources. First, Hoffman et al. (83) observed two polarographic waves of one electron each for the reduction of t-butyl iodide. Using t-butyl bromide, only one two electron polarographic wave was obtained. The second source is indirect evidence such as the formation of organometallics (84) at mercury (85,86), at lead (87,88), and at tin (89). The formation of coupled products is suggested to be indicative of free radical reactions although an S_N2 reaction of an electrochemically generated carbanion on alkyl halide starting material can not be exclusively ruled out. Brown (85) argues that dimers are formed from the organomercury products which form from a free radical attack on mercury. Fleischmann et al. (89) rule out the carbanion attack on RX as being responsible for coupled product on the basis that if such an attack occurs for one reaction, it should occur for all alkyl halides. This latter argument can be attacked by noting that the reduction of alkyl

halide is potential dependent (90), see Table III. The products generated are related to the working electrode potential therefore such a naive statement ignores the complexity of the problem.

Evidence for carbanions comes from coulometric work, trapping by CO_2 to form carboxylic acids (68), or by isolation of the Hofmann elimination products (76) when the solvent is aprotic.

$$R^- + CH_3CH_2\overset{(+)}{N}Et_3 \rightarrow RH + CH_2{=}CH_2 + 2Et_3N$$

Organometallic Electrochemistry

The synthesis of organometallic compounds has already been suggested to provide evidence of free radical formation during the reduction of organic halides (84-89). Settineri and McKeever (91) and Lehmkuhl (90,92) have reviewed the area of synthetic organometallic electrochemistry and the subsequent electrochemical degradation of the organometallic has been reviewed by Dessey (93).

The electrochemical formation of organometallics can proceed via one of three routes (90,92).

1. The reduction of organic compounds to form organic radicals which subsequently attack the cathode metal to form the organometallic (sacrificial cathode).

2. Metallic compounds can be reduced to a lower valence state of the metal. As noted in the introduction, this state is often not

Table III. Cathode Potential versus Product Distribution (90)

C Potential V vs Ag/AgCL	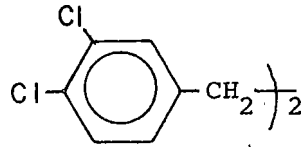 %	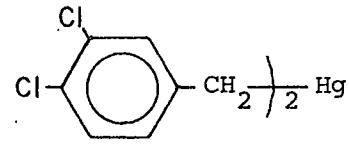 %
-0.94	2.1	39.0
-1.05	25.0	26.6
-1.30	21.0	4.6

stable per se but may be stabilized by suitable organic complexing agents.

3. Anodic oxidation of organometallics containing carbanions to generate free radicals which can then attack the anode material to form new organometallics.

The reductive routes of organometallic synthesis are particularly germain to this problem. The proposed scheme to account for the organometallic products formed at a sacrificial cathode is (86,87)

$$RX + 1e^- \rightarrow R^{\bullet}_{ads} + X^- \xrightarrow{1e^-} R^- \xrightarrow{H^+} RH$$

$$R^- \xrightarrow{M_{cathode}} RM$$

The formation of the organometallic is a function of the cathode potential as noted in Table III. The major tools used to identify reduction pathways for organic halides has been polarography with a dropping mercury electrode and controlled potential electrolysis using a mercury cathode or some other sacrificial electrode. Brown (85) claims that simple dimers are seldom formed as the major product of halide reduction and, when they are reported, they have been formed from organomercury products during the analysis after the reduction. This view is particularly harsh, but does suggest that "free" radicals are adsorbed radicals and the lifetime of a carbanion

is too short even in aprotic solvents to engage in nucleophilic attack on the starting material.

The formation of organometallic compounds by reducing the metal in the presence of an organic substrate has led to the preparation of several organometallic complexes. Usually the organic ligand is a complexing agent with multiple π-bonds which are effective in stabilizing low valent metals. Several examples follow.

$$Fe(acac)_3 \xrightarrow[\text{stainless steel cathode}]{\text{reduction}\ CO,\ 86^\circ} Fe(CO)_5 \quad 65\% \qquad (94)$$

$$Ni(acac)_2 \xrightarrow{\text{Al-anode, THF}} \frac{1}{n}[Ni(C_8H_8)]_n + \frac{2}{3}Al(acac)_3 \qquad (90)$$

$$Ni(acac)_2 \xrightarrow[Ph_3P]{\text{Al-anode, THF}} Ni(PPh_3)_4 + \frac{2}{3}Al(acac)_3 \qquad (90)$$

$$CO(acac)_2 \xrightarrow[\text{THF}]{\text{1) +2e, Al anode}} CH_2{=}CH\underset{\underset{CH_3}{|}}{C}H{-}CH{=}CH{-}CH{=}CH_2 +$$

$$\text{2) butadiene}$$

$$CH_2{=}CH{-}CH{=}CH{-}CH_2{-}CH_2{-}CH{=}CH_2 \qquad (90)$$

The latter example represents a reaction that has led to the dimerization of butadiene via a reduced form of cobalt and assumed organocobalt intermediate.

The formation of organometallics is important in systems where they are assumed to be generating product. Dessy's work on the electrochemical degradation of the organometallics is shown in Figure 5 (90,93). Lehnkuhl (90) has given examples of these routes and the reader is referred to his article.

Electrochemical Cells

The methodologies for examining an electrochemical reaction have been discussed by Headridge (95), Sawyer and Roberts (96), Cauguis (97), Meites (98), and Fry (68). Fundamental electrochemical concepts are thoroughly developed by Bockris and Reddy (99) and the reader is referred to this text for detailed study.

Of the available electrochemical techniques used to examine an electrochemical system, the least articulate is macroscopic synthesis. The transition from microelectrochemistry to macroelectrolysis cells is not necessarily smooth for it involves increasing the concentration of the electrophore 100 to 10,000 times that used in a polarographic technique (100). The practical problems of electrolysis on large samples have been reviewed (101).

Three types of electrolysis cells are available for large scale electrolysis. Two of these cells are two-electrode assemblies which operate at either constant current or constant applied potential. The third cell is referred to as a three-electrode cell. Its operation

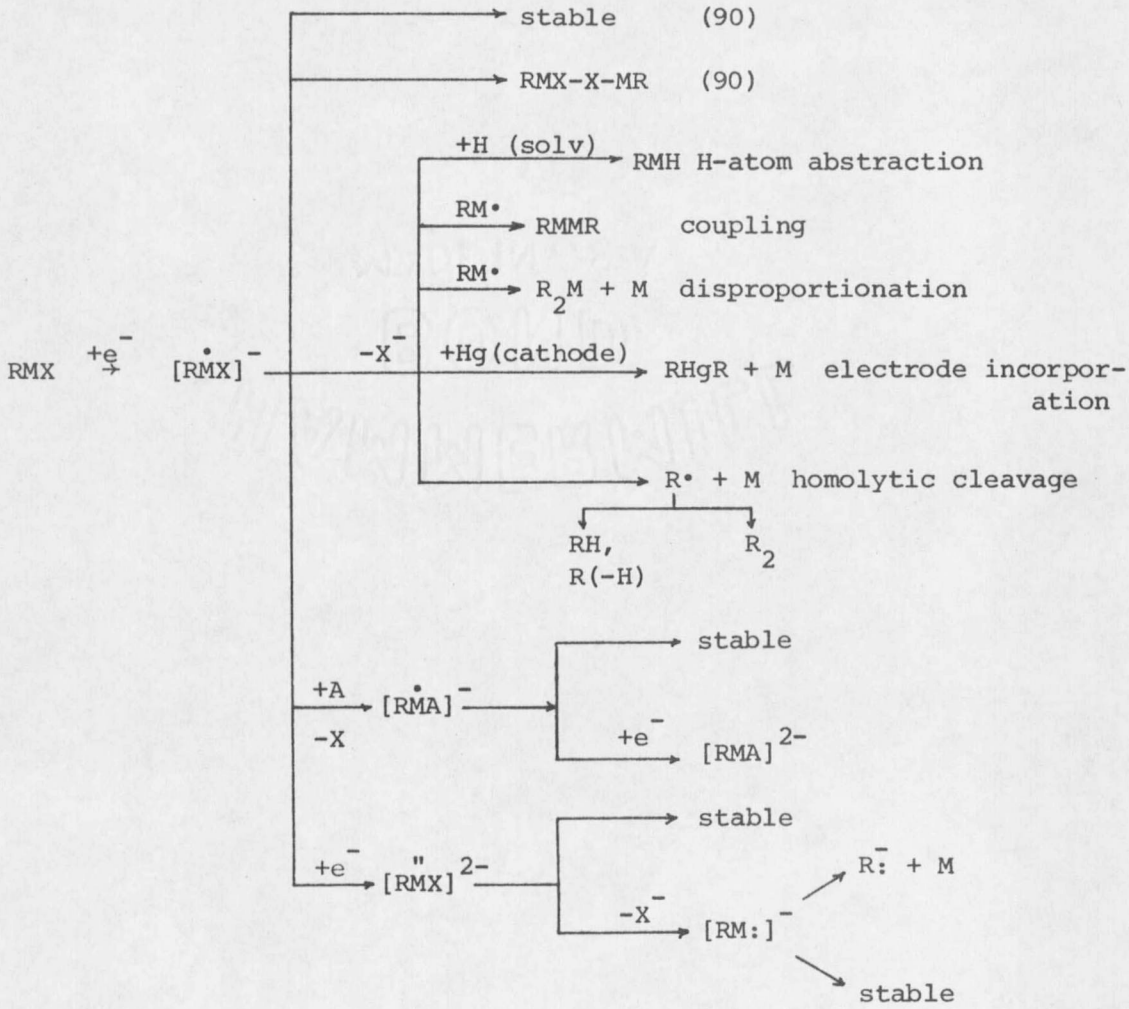

Figure 5. Electrochemical Degradation of Organotransition Metals (90,93).

involves the control of the working electrode potential (102). All three cell types have been used in this work and a more thorough presentation will be given in the discussion.

Statement of the Problem

Two advantages which an electrode has over a chemical reducing agent are (1) control of the reduction potential of the electrode which then introduces energy selectively into a system and hence varies the number of electrons transferred, and (2) the electrode often simply adds or removes an electron from the electrophore without entering into bonding as is often the case with chemical reagents (103). An electrochemical cell will be used to examine the plausibility of generating low valent metal ions or atoms in the presence of an organic halide. The organic halide can subsequently react with the low valent metal according to the homogeneous processes outlined in the introduction. The strategy is to selectively reduce the metal ion without concommitant electrochemical reduction of the organic halide thus the inorganic ion functions as a homogeneous mediator in the overall conversion of organic halide to products (104).

$$\text{Reduced inorganic ion} + RX \rightarrow \text{Oxidized inorganic ion} + \text{products}$$

$$\underbrace{\text{Oxidized inorganic ion} \xrightarrow{+\,ne^-} \text{Reduced inorganic ion}}_{\text{Cathode}}$$

DISCUSSION

Two-Electrode Systems

The reaction we are attempting to effect is the conversion of alkyl halides to coupled dimer, R_2, and disproportionated products, RH and R(-H) where RH represents an alkane and R(-H) the olefin. This transformation is known to occur

$$RX \xrightarrow{[M]} [R_2, RH, R(-H)]$$

in several organic reactions using reduced forms of the metal such as the classical Wurtz reaction and the Kharasch reaction.

Our initial investigations into this transformation used a two-electrode cell run under constant current or constant applied potential (66,105). Table IV indicates that coupled products were formed during the reaction. The cell used in this phase of the examination is shown in Figure 6. The operation of the two electrode cells under constant current and constant applied potential will be considered.

Two solution electrophores are available for reduction in the electrolysis cell, the metal ion and the organic substrate. Each electrophore has its own reduction potential corresponding to $E^{M}_{1/2}$ and $E^{RX}_{1/2}$ where M and RX represent the metal ion and the organic halide, respectively. Figure 7 shows a possible polarographic trace for two solution electrophores. A judicious selection of metal ion and organic halide will generate a cell in which the metal is reduced before the organic

Table IV. Coupling of Organic Halides (105)

Substrate	Metal Acetylacetonate	Electrode (Cathode/Anode)	Stabilizing Ligand	Product	% Yield
1-Bromobutane	Fe	Ni/Ni	Ph_3P	Octane	28
2-Bromobutane	Fe	Ni/Ni	Ph_3P	3,4-Dimethyl hexane	20
2-Bromo-2-methyl-butane	Fe	Ni/Ni	Ph_3P	No coupling	
1-Octylbromide	Fe	Al/Al	Ph_3P	Hexadecane Octane 1-Octene	32 11 3
1-Octyl bromide	Fe	Al/Al	—	Hexadecane Octane 1-Octene	30 49 18
Benzyl chloride	Ni	Cu/Ni	Ph_3P	Bibenzyl	87
Benzyl bromide	Ni	Cu/Ni	Ph_3P	Bibenzyl	85
Phenyl bromide	Ni	Cu/Ni	Ph_3P	Biphenyl	65

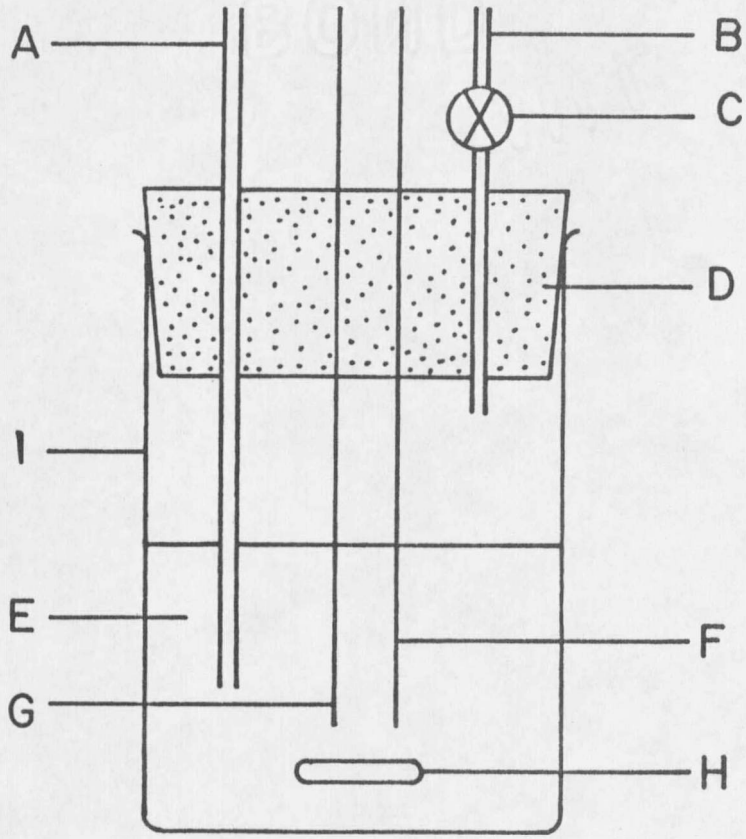

Figure 6. Two-electrode Electrolysis Cell: (A) nitrogen inlet for purging the solution and maintaining a positive pressure; (B) gas outlet which is open during purging and closed during electrolysis; (C) stopcock for closing gas outlet; (D) rubber stopper; (E) electrolysis solution; (F) cathode; (G) anode; (H) magnetic stirring bar; (I) 100-ml Berzelius beaker.

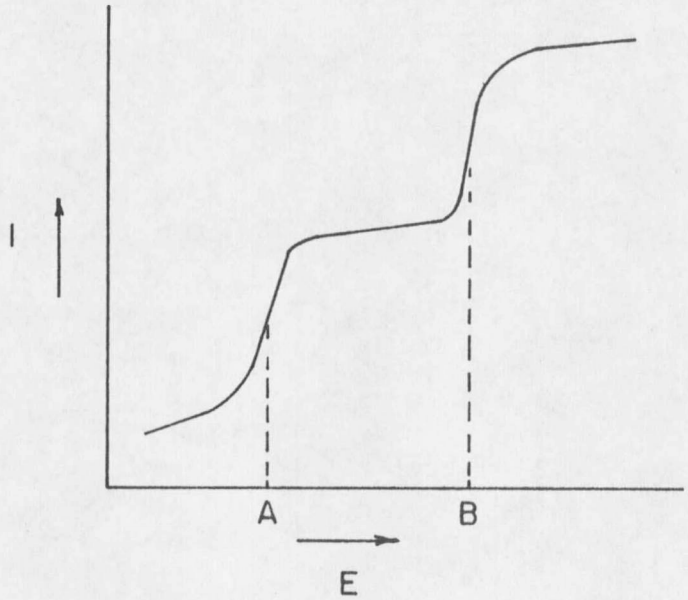

Figure 7. Polarogram for Two Electrophores. I is current, E is potential of dme versus suitable reference, A is $E_{1/2}$ of metal ion, B is $E_{1/2}$ of alkyl halide.

substrate, $E^{M}_{1/2} > E^{RX}_{1/2}$. Although the polarographic cell operates with solution concentrations of 10^{-4} M, the macroscopic cell using concentrations of 1.0 to 0.1 M is expected to behave similarly, that is $E^{M}_{1/2} > E^{RX}_{1/2}$. Figure 8 presents an I-E curve for such a macroscopic system containing two reducible electrophores (101). When the cathode potential is less than E_A no current will flow through the cell since no electron transfer reactions occur across the electrode-solution interface. When the potential of the cathode reaches E_A, current begins to flow. As the potential of the cathode is adjusted from E_A to E_B, the current increases with the changing potential much like that observed in a polarographic cell. The current in this region is potential dependent. Between potentials E_B and E_C, the current is independent of the cathode potential and the electrode is said to be polarized. All of the molecules or ions of the electrophore that arrive at the electrode and can undergo this reduction are reduced as soon as they reach the electrode. The current associated with this plateau is the limiting current, i_d. Continued cathodic shifts past E_C result in the reduction of the second electrophore.

Constant current electrolysis is also demonstrated in Figure 8. If a current is selected such that the control current, i_o, is less than the limiting current, i^{I}_{d}, for the first reduction, the electrophore corresponding to the first curve--in this example the metal ion --is reduced. This is the idealized system envisioned to be occurring

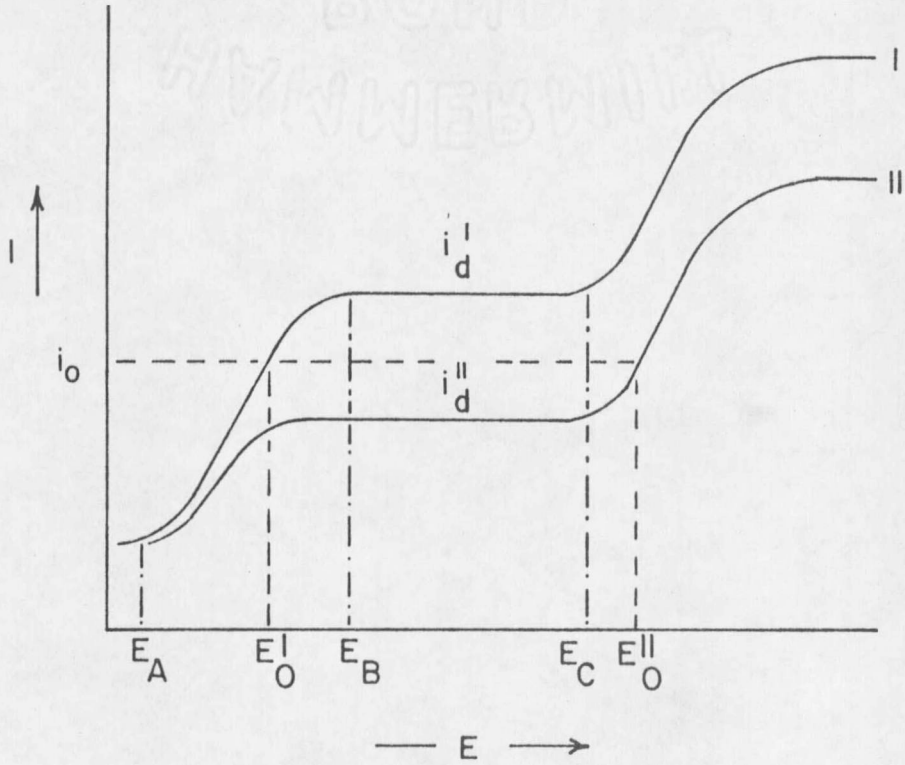

Figure 8. Macroscopic Cell with Two Solution Electrophores (101).

within the electrolysis cell. The cathode potential for this current level is E_O^I. As the electrolysis continues, the concentration of the metal ion decreases resulting in a decrease in magnitude of the limiting current for the metal ion, i_d^{II}. However, i_d^{II} is less than the preselected current, i_o, therefore the cathodic potential must shift to E_O^{II} in order to compensate for the current difference between i_d^{II} and i_o. This shift in the cathodic potential with the concommitant increase in the current in order to maintain the current level, i_o, means that another solution electrophore is being reduced. In the system under investigation, this reflects the direct reduction of the organic substrate. The strategy of selective reduction of the metal ion is forfeited.

Figure 8 depicts an ideal system in which the cathode potential E_C, is being followed. Without a reference electrode in the system, the cathodic potential is not known. The potential that is observed to change in a two electrode cell is the applied potential. This change in the applied potential is not necessarily a simple function of the current as indicated for the cathodic process in Figure 8. The applied potential is a function of several components given by the equation (106)

$$E_{APP} = E_C - E_A - iR - E_{overpotential}$$

where E_{APP} is the applied potential, E_C is the cathode potential, E_A the anode potential, iR the potential drop due to the resistance of the

solution to current passage, and $E_{overpotential}$ is the voltage in excess of the theoretical value for the cell calculated from the Nernst equation that is required to get the electrolytic reaction to occur at an appreciable rate. Both the overpotential and the solution resistance can change during the electrolysis, the changes not being fundamentally related to the cathodic potential or the overall current. For instance, the conductivity of the solution might increase if the anode reaction is a discharge (oxidation) of a metal. This could cause the applied potential to be reduced in a constant current cell since the resistance of the solution is reduced. Likewise, the overpotential may be less as the surface of the cathode undergoes modification such as occurs in plating a solution ion onto an inert electrode. This would result in a decrease in the applied potential even though the current is held constant.

The problems of the two-electrode cell run at constant current are not completely removed when the system is operated using two electrodes at constant applied potential. V. T. Brice initiated the study using constant applied potential (105). Under this method of operation, the potential applied across the two electrodes is held at some constant value. The current-time behavior for this type of cell using an aqueous solution and the simple reduction

$$Ox + ne^- \rightarrow Red$$

is shown in Figure 9. The current for such a simple reduction is expected to decay in an exponential manner. This current decay is described by a logrithmic function in terms of current or concentration of the electrophore (68).

$$\log i_t = -\beta t + \log i_{lim}$$

or

$$\log C^{*,t} = -\beta t + \log C^*$$

where i_t is the current at time t and i_{lim} is the limiting current for the initial concentration of the electrophore, C*. The bulk solution concentration at time t is given by $C^{*,t}$. Beta is referred to as the electrochemical rate constant. Beta is a function of several parameters

$$\beta = \frac{0.43\ DA}{V\delta}$$

where D is the diffusion constant for the electrophore, A is the surface area of the electrode, V is the volume of the electrolysis solution, and δ is the Nernst diffusion layer thickness. Controlling the magnitude of these terms can generate a faster electrolysis. Figure 9 shows two curves for the same concentration of an electrophore in two different cells. Curve A represents a cell of high β and consequently short electrolysis times. Curve B represents a curve of much smaller

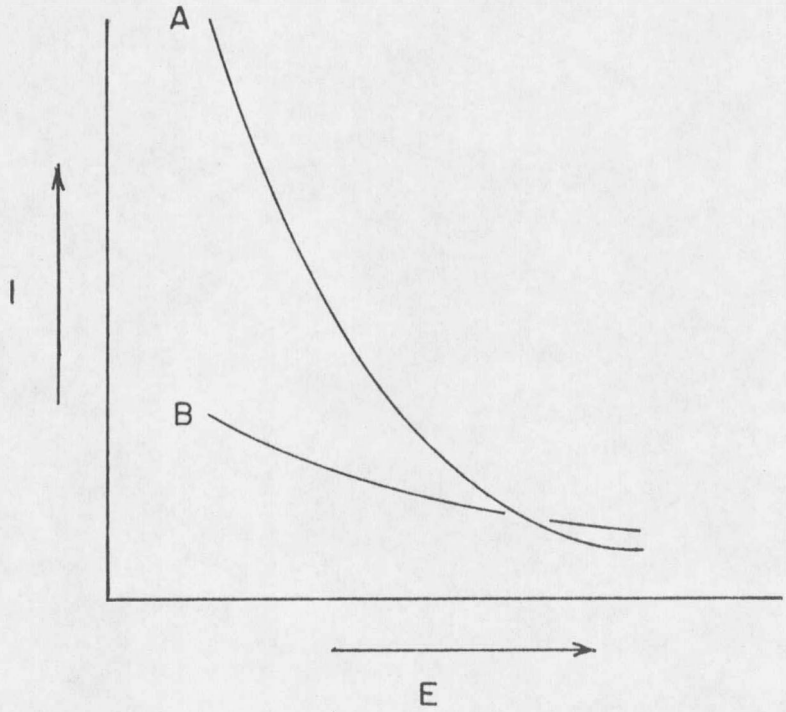

Figure 9. Current-Time Curves for Two Systems with Different Electrochemical Rate Constants (68).

β and hence longer electrolysis times. The general characteristics for both curves is a smooth decay of the current with time.

For the ideal case in a constant applied potential electrolysis cell, the current falls smoothly with time. Such ideality is not always available. Recall that the total applied potential of the electrolysis cell not only includes the potential difference of the cathode and the anode, but also the internal resistance and overpotential of the cell. The internal resistance of an aqueous solution with a high concentration of a base electrolyte is normally not very large. Thus $E_{cathode} - E_{anode}$, the thermodynamic cell potential, is not very different from $E_{Applied}$ if the overpotential for the particular reaction is small. However, for nonaqueous solutions, the high internal resistance of the solvent influences the magnitude of the applied potential. Hence the thermodynamic potential and the applied potential are not so readily related. Should the internal resistance change during the electrolysis, E_{anode} and $E_{cathode}$ must also change in order to maintain a constant applied potential. If the nature of the cathode changes during reduction as it can if plating occurs, the overpotential of the new surface may be less than the overpotential of the original surface. If the cathodic potential for this new surface does not change, that is the applied constant potential holds this new surface at the same potential as the old surface, the permissible current density at the new surface can vary widely (107) or an entirely new

electrolysis reaction can occur. This effect of the electrode material on the overpotential for hydrogen gas evolution is demonstrated in Table V. As the exchange current density decreases, a greater applied potential is required to reduce the proton to H_2 at an appreciable rate.

Table V. Approximate Exchange Current Densities for the Hydrogen Reaction on Metals at 25°C (108)

Metal	Exchange Current Density (A/cm^2)	Metal	Exchange Current Density (A/cm^2)
Pb,Hg	10^{-13}	Fe,Au,Mo	10^{-6}
Zn	10^{-11}	W,Co,Ta	10^{-5}
Sn,Al,Be	10^{-10}	Pb,Rh	10^{-4}
Ni,Ag,Cu,Cd	10^{-7}	Pt	10^{-2}

The two-electrode cell run under constant applied potential does provide some information concerning the reaction being investigated. The system used as a probe into the nature of the electrochemical reaction incorporated iron (III) acetylacetonate, $Fe(acac)_3$, as the inorganic transition metal salt and 1-octyl bromide as the organic substrate. The results in Table IV indicated that the organic products for this reaction were hexadecane, (R_2), n-octane (RH), and 1-octene, [R(-H)]. Triphenylphosphine, Ph_3P, was used in the cell for two purposes. Kochi (41) noted a greater amount of dimerization occurs for those favorable systems in the Kharasch reaction when Ph_3P

was present than when it was absent. Secondly, the weak π-back bonding ability of the Ph_3P can help stabilize and solubilize the reduced forms of the iron by removing some of the electron density from the reduced iron.

Table VI presents additional results obtained with this two-electrode cell for the reduction of $Fe(acac)_3$ in the presence of 1-octyl bromide. Several points should be noted. First, the yields of hexadecane, octane, and 1-octene are based on the amount of unrecovered starting material. The per cent reaction represents how much of the starting material was consumed. Summing the yields of recovered products demonstrates that not all of the unrecovered material is accounted for. Secondly, the suggested general reaction does appear to occur with 1-octyl bromide generating dimer, alkane, and olefin. Finally, the reactions listed in Table VI were prepared so that all the systems were identical. However, the yields of products are rather widespread. In one instance, no products were obtained yet in another identical reaction as much as 33% coupling occurred. Obviously, the reproducibility of the system is questionable.

Current-time traces for three representative experiments obtained from the two-electrode constant applied potential cell are given in Figure 10. Although these cells are assembled so that the solution concentrations are duplicated, the current-time behavior suggests that the reactions occurring in the solutions are not identical. The

Table VI. Product Yields for the Two-Electrode Constant Applied Potential Electrolysis Cell with Octyl Bromide and $Fe(acac)_3$ using Aluminum Electrodes.

Reaction No.	NI025	NI085	NI114	NI118	NI127
% $C_{16}H_{34}$	0	27.6	20.7	23.9	25.4
% C_8H_{18}	0	} 9.6	17.2	10.1	7.7
% C_8H_{16}	0		6.2	4.1	4.3
% Reaction	None	100%	100%	100%	100%
I_{max} (mA)	15	42	42	37	22
Δt (hours)	76½	92½	88½	91	114

Reaction No.	NI147	NI170	NI190	NI193	NII033
% $C_{16}H_{34}$	32.4	31.9	33.8	2.5	9.5
% C_8H_{18}	11.1	28.5	30.8	12.0	6.3
% C_8H_{16}	3.2	7.0	9.1	1.9	2.6
% Reaction	72.3	59.9	64.5	34.2	64.2
I_{max} (mA)	37	32	36	16	36
Δt (hours)	65	73	73	124	119½

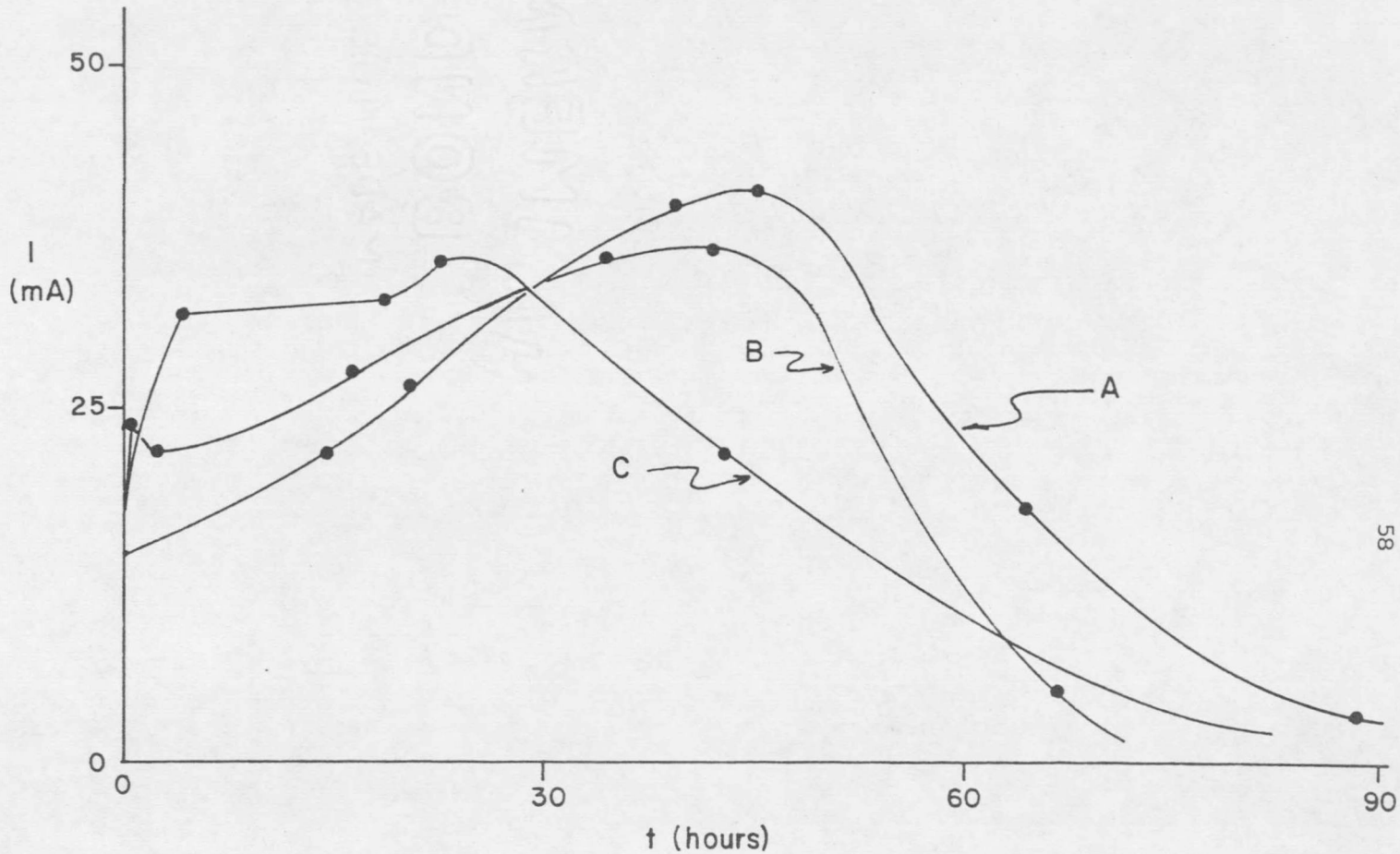

Figure 10. Current-Time Behavior for Three Representative Two-Electrode Constant E_{APP} Electrolysis Cells with Aluminum Electrodes. (A) Reaction NI114; (B) Reaction NI118; (C) Reaction NII033. E_{APP} = 1.5V for each reaction.

current-time behavior is not typical. The rise in current is unexpected for a simple reduction of a metal ion electrophore in an constant applied potential electrolysis cell.

Several possible systems could account for this current-time behavior. Two trivial situations are associated with the method of electrolysis. The aluminum electrode is covered with an oxide layer before immersion into the electrolysis cell. This is an insulating layer which may be removed during the electrolysis. Alternatively, the aluminum electrodes are rendered passive when placed into the electrolysis cell. Such passivation of the aluminum is known to occur with amines (109). Activation of the electrode is demonstrated by a current rise. The increase in current during the initial electrolysis could also indicate a change in either the internal resistance of the solvent or a change in the reaction overpotential or both. The anticipated change would be a reduction in the resistance and/or overpotential so that the potential drop between the cathode and the anode increases. This is analogous to making the cathode potential more negative (cathodic). Such a drift in the cathode potential could increase the current in two ways. First, if the initial cathode potential is near the foot of the reduction wave corresponding to point E_A in Figure 8, the negative drift in the cathode potential would cause the current to increase. Alternatively, this potential drift is sufficiently cathodic to initiate the reduction of a second solution

electrophore. Finally, if iron is plating onto the aluminum electrode and the overpotential for reducing iron ions at an iron surface is lower than the overpotential for reducing iron ions at an aluminum electrode, the current would again increase. Alternatively, the direct electrochemical reduction of the 1-octyl bromide may proceed at this newly plated iron surface although it would not have occurred at the aluminum electrode. This latter situation conflicts with the reaction strategy. As noted in the introduction, such direct reductions of the organic halides are not known to lead to coupled products, therefore this latter situation is not expected to be occurring in the reactions of Table VI.

A reference electrode was used to monitor the cathode potential in the two-electrode constant applied potential electrolysis cell. Figure 11 shows that the cathode potential does shift during the electrolysis.

Ideally, the increase in current may be indicative of a chemical reaction occurring after the initial electron transfer step. The original view postulated by Pillsbury (66) with some slight modifications associated with this research is contained in Figure 12. This postulated reaction scheme generates a reducible form of iron, $Fe^{II}X_2L_{n-2}$ during the cycle going from reduced to oxidized iron which is mediated by the 1-octyl bromide. The original iron salt, $Fe(acac)_3$, has a bidentate ligand attached to the metal center. Iron (III) may be easily